The Journal of Immunology

The Development and Function of Memory Regulatory T Cells after Acute Viral Infections

Ana M. Sanchez, Jiangao Zhu, Xiaopei Huang and Yiping Yang

J Immunol 2012; 189:2805-2814; Prepublished online 1 August 2012;
doi: 10.4049/jimmunol.1200645
http://www.jimmunol.org/content/189/6/2805

The Journal of Immunology is published twice each month by
The American Association of Immunologists, Inc.,
1451 Rockville Pike, Suite 650, Rockville, MD 20852

Print ISSN: 0022-1767 Online ISSN: 1550-6606.

The Development and Function of Memory Regulatory T Cells after Acute Viral Infections

Ana M. Sanchez,* Jiangao Zhu,† Xiaopei Huang,† and Yiping Yang*,†

Natural CD4$^+$CD25$^+$Foxp3$^+$ regulatory T cells (Tregs) are critical for the control of immune responses to pathogens. However, most studies have focused on chronic infections, in which pathogen-specific Tregs contribute to pathogen persistence and, in some cases, concomitant immunity. How Tregs behave and function following acute infections remains largely unknown. In this article, we show that pathogen-specific Tregs can be activated and expand upon acute viral infections in vivo. The activated Tregs then contract to form a memory pool after resolution of the infection. These memory Tregs expand rapidly upon a secondary challenge, secrete large amounts of IL-10, and suppress excessive immunopathological conditions elicited by recall expansion of non-Tregs via an IL-10–dependent mechanism. Our work reveals a memory Treg population that develops after acute viral infections and may help in the design of effective strategies to circumvent excessive immunopathological effects. ***The Journal of Immunology*****, 2012, 189: 2805–2814.**

Naturally occurring CD4$^+$CD25$^+$ regulatory T cells (Tregs) are a cell lineage devoted to the maintenance of homeostasis in the immune system. The natural Treg lineage develops in the thymus and exits to the periphery, where these cells represent 5–10% and 2–4% of the CD4$^+$ T cell population in healthy mice and humans, respectively (1, 2). They are phenotypically characterized by the expression of the IL-2R α-chain (CD25), CTLA-4, glucocorticoid-induced TNFR (GITR), and high levels of folate receptor 4 (FR4) (3–5). The most definitive signature of natural Tregs, however, is the expression of the transcription factor Foxp3, which is required for Treg development and function (6–8).

Functionally, Tregs are defined by their ability to suppress the activation of multiple cell types, including CD4$^+$ and CD8$^+$ T cells, B cells, NK cells, and dendritic cells (9–13). Suppression can be achieved by the production of immunosuppressive cytokines, by direct cell-to-cell contact, or by modulating APCs (14). The suppressive ability of natural Tregs is crucial in maintaining dominant tolerance—the active, *trans*-acting suppression of the immune system for the prevention of autoimmune diseases. This critical role of natural Tregs has been exemplified by studies wherein functional deletion of Tregs leads to aggressive and fatal autoimmune diseases (15–17). Dysregulation of Tregs is associated with other autoimmune diseases, including, but not limited to, multiple sclerosis, type 1 diabetes, and rheumatoid arthritis (18–20). Studies have also demonstrated a critical role for the natural Treg in downmodulating antitumor immunity, suppressing allergic diseases such as asthma, and achieving transplant tolerance (21–23).

Accumulating evidence has also suggested an important role for Tregs in the control of immune responses to pathogens (24, 25). The overwhelming majority of these studies have focused on chronic infections, in which the presence of Tregs controls effector immune responses, affecting disease outcome in a variety of ways. By downmodulating the immune response, Tregs can function to reduce immune-mediated disorders, as demonstrated in models of pulmonary inflammation caused by *Pneumocystis* pneumonia, inflammatory eye lesions with HSV, and liver disease in *Schistosoma mansoni* infection (26–28). In addition to reducing immunopathological conditions, the presence of Tregs can lead to pathogen persistence. However, the presence of Tregs can also be beneficial to the host by maintaining protective immunity. Specifically, in models of *Leishmania* infection, *Leishmania*-specific Tregs found at the site of infection prevent pathogen clearance, which is critical for the development of concomitant immunity (29, 30).

In contrast to chronic infections, how Tregs behave and function during acute infections remains largely undefined. In this article, we show that pathogen-specific Tregs can be activated and expand upon acute infections with vaccinia virus (VV) or influenza virus in vivo. Similar to non-Treg CD4$^+$ T cells, activated Tregs undergo contraction to form a memory pool after resolution of the infection. These memory Tregs can rapidly expand, secrete high levels of IL-10, and suppress the collateral tissue damage and inflammation elicited by recall expansion of non-Treg memory CD4$^+$ T cells. These results suggest that development of a memory Treg population following an acute infection may help prevent excessive immunopathological effects during a recall response. Furthermore, we provide evidence that the ability of memory Tregs to suppress memory non-Treg CD4$^+$ T cells during a recall response is dependent on IL-10.

Materials and Methods

Mice

B10.D2 and BALB/c mice were purchased from The Jackson Laboratory (Bar Harbor, ME). The 6.5 HA-TCR transgenic mice on BALB/c background that express a TCR recognizing an I-E^d–restricted hemagglutinin (HA) epitope (^{110}SFERFEIFPKE^{120}) were kindly provided by Dr. H. von Boehmer (Harvard University, Boston, MA). These mice were backcrossed onto the Thy1.1$^+$ B10.D2 background (31). Mice expressing enhanced GFP under control of the endogenous Foxp3 promoter (Foxp3-GFP knockin mice on BALB/c background) were purchased from The Jackson Laboratory. These mice were intercrossed with 6.5 HA-TCR trans-

*Department of Immunology, Duke University Medical Center, Durham, NC 27710; and †Department of Medicine, Duke University Medical Center, Durham, NC 27710

Received for publication February 23, 2012. Accepted for publication July 12, 2012.

This work was supported by National Institutes of Health Grants CA111807, CA047741, CA136934, AI079366, and AI083000 (to Y.Y.).

Address correspondence and reprint requests to Dr. Yiping Yang, Department of Medicine, Duke University Medical Center, Box 103005, Durham, NC 27710. E-mail address: yang0029@mc.duke.edu

Abbreviations used in this article: Ad-HA, recombinant adenovirus encoding HA; HA, hemagglutinin; T_{CM}, central memory T cell; T_{EM}, effector memory T cell; Treg, regulatory T cell; VV, vaccinia virus; VV-HA, recombinant VV encoding HA.

www.jimmunol.org/cgi/doi/10.4049/jimmunol.1200645

genic mice to generate 6.5 HA-TCR Foxp3-GFP mice. All mice used in these studies were between 8 and 12 wk of age. Experimental procedures were performed in accordance with protocols approved by the Animal Care and Use Committee of the Duke University Medical Center.

Adoptive transfer of HA-specific transgenic T cells

Naive clonotypic HA-specific Treg and non-Treg CD4$^+$ T cells (Thy1.1$^+$) were prepared from 6.5 HA-TCR transgenic mice, as described (32). CD25$^+$ T cells were enriched by MACS-positive selection by staining with PE-conjugated anti-CD25, followed by anti-PE MicroBeads (Miltenyi Biotec). CD25$^+$ cells were selected using a MACS column (Miltenyi Biotec) according to the manufacturer's instructions. Following this procedure, unbound cells (CD25$^-$ enriched) were sorted, gating on 6.5$^+$CD4$^+$ CD25$^-$ cells (non-Treg), and CD25$^+$-enriched cells were sorted, gating on 6.5$^+$CD4$^+$CD25$^+$ cells (Treg), with a FACSVantage (BD Biosciences) high-speed cell sorter. The purity of FACS-sorted populations of cells was >98%. After sorting, 1×10^5 cells (Treg or non-Treg) were transferred into recipient B10.D2 mice (Thy1.2$^+$) i.v. in 200 μl HBSS.

Viruses

Recombinant VV encoding HA (VV-HA) and recombinant E1-deleted adenoviruses encoding HA (Ad-HAs) were previously described (32). Mice were infected with 2×10^6 PFU VV-HA i.p. or 5×10^5 PFU intranasally, or 2×10^9 PFU Ad-HA i.v. Influenza A/PR/8/34 (H1N1) was obtained from American Type Culture Collection (Manassas, VA). The viral titer was determined by a plaque assay, as previously described by Lin et al. (33). Immediately prior to intranasal administration of the influenza, mice were anesthetized with 3% isoflurane. Then 40 μl 4000 tissue culture-infective dose, at 50%, of influenza in sterile PBS was instilled intranasally.

Abs and flow cytometry

Abs for staining were PE-, FITC-, and APC-conjugated anti-CD4; PE- and PerCP-conjugated anti-Thy1.1; APC-conjugated anti–IFN-γ; biotinylated anti-CD62L; PE-conjugated anti-CD44; PE-conjugated anti–IL-10; streptavidin-PeCy5; and PE-conjugated anti-CD25 (all from BD Biosciences). FITC-conjugated anti-Foxp3 was purchased from eBioscience. Anti–TCR-HA Abs (6.5) were purified and conjugated in our laboratory. Collection of flow cytometry data was carried out using a FACSCanto (BD Biosciences), and events were analyzed using FACSDiva software (BD Biosciences).

For intracellular Foxp3 staining, 1×10^6 cells were surface stained, and then fixed/permeabilized using the Cytofix/Cytoperm Kit (BD Biosciences) according to the manufacturer's instruction. Following fixation, cells were stained with FITC-conjugated anti-Foxp3. For intracellular IFN-γ and IL-10 staining, cells were cultured for 6 h in the presence of 5 μg/ml GolgiPlug (brefeldin A; BD Biosciences) and 20 μg/ml I-E^d–HA peptide.

Histopathology and immunohistochemistry

For histopathological study, tissues were harvested and prepared for paraffin sections and cryosections. Paraffin sections (5 μm) were stained with H&E according to standard procedures. Random sections were examined for

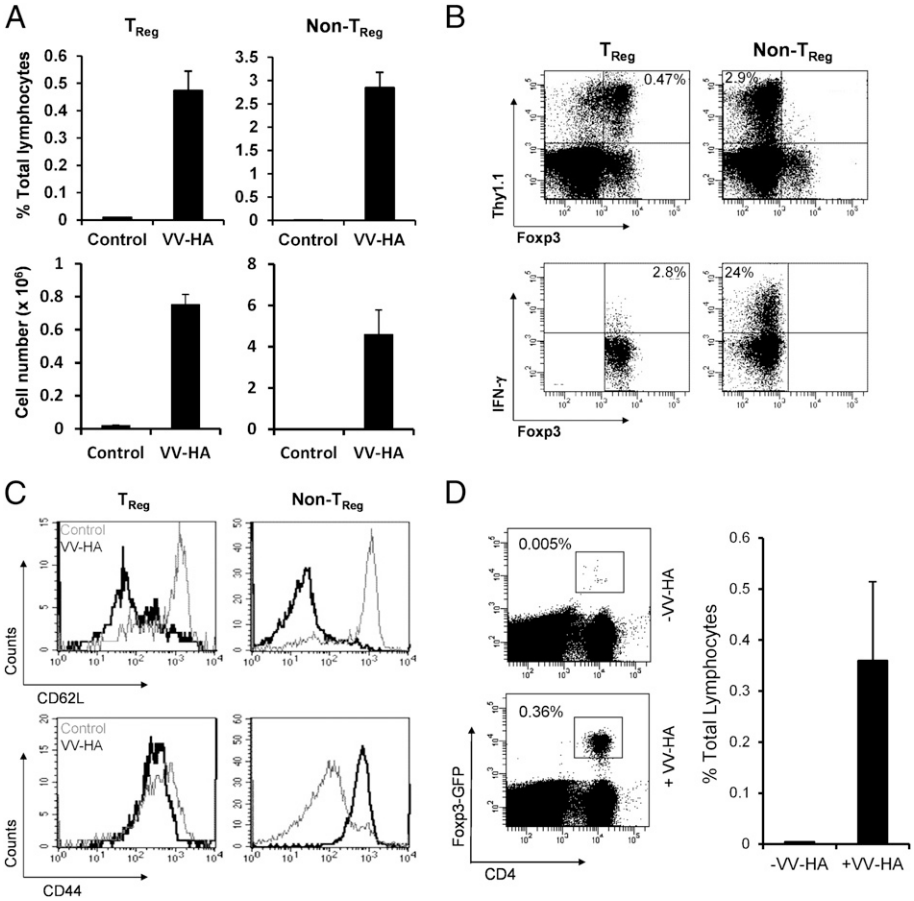

FIGURE 1. Activation and expansion of pathogen-specific Tregs upon an acute viral infection. Purified naive HA-specific Tregs or non-Tregs (Thy1.1$^+$) were transferred into B10.D2 mice (Thy1.2$^+$) and subsequently infected with VV-HA or left uninfected as a control. At 7 d post infection, mice were harvested for the following analyses. (**A**) Splenocytes were stained with anti-CD4, anti-Thy1.1, and anti-Foxp3, and the mean percentages of Tregs (CD4$^+$ Thy1.1$^+$Foxp3$^+$) or non-Tregs (CD4$^+$Thy1.1$^+$Foxp3$^-$) among total lymphocytes, as well as their absolute cell numbers, were plotted with the standard deviations included. (**B**) Splenocytes were stained with anti-CD4, anti-Thy1.1, anti-Foxp3, and anti–IFN-γ. The percentage of Tregs or non-Tregs among total lymphocytes is indicated (*top panels*). The percentage of IFN-γ$^+$ Tregs among CD4$^+$Thy1.1$^+$Foxp3$^+$ Tregs and that of IFN-γ$^+$ non-Tregs among CD4$^+$ Thy1.1$^+$Foxp3$^-$ non-Tregs are indicated (*bottom panels*). (**C**) Splenocytes were stained with anti-CD4, anti-Thy1.1, anti-Foxp3, and anti-CD62L or anti-CD44 and subjected to FACS analysis. (**D**) Purified Foxp3-GFP$^+$ TCR-HA$^+$ Tregs were transferred into BALB/c mice, which were subsequently infected i.p. with VV-HA (+VV-HA) or left uninfected (−VV-HA) as a control. At 7 d post infection, splenocytes were harvested and stained with anti-CD4. The percentage of Foxp3-GFP$^+$ donor Tregs among CD4$^+$ T cells is shown. Results are representative of three independent experiments.

histopathological changes in a blinded fashion, using the criteria we described previously for adenoviral hepatitis, with minor modifications (34).

For immunohistochemistry, frozen sections (5 μm) were acetone fixed and then stained with FITC-conjugated anti-CD4, followed by Alexa Fluor 488-conjugated anti-FITC and Alexa Fluor 546-conjugated H36 (anti-HA mAb, kindly provided by Dr. W. Gerhard, Wistar Institute, Philadelphia, PA). With use of a Zeiss fluorescence microscope, the number of $CD4^+$ cells in each section was quantified by counting $CD4^+$ cells found in ten randomly selected fields of view.

In vivo blocking of IL-10R, TGF- β, and CTLA-4

For in vivo blocking of IL-10R, TGF-β, and CTLA-4, mice were injected with blocking Abs 6 h before infection with VV-HA intranasally, as well as 2 d following Ag rechallenge. The following Abs were used: 0.5 mg anti–IL-10R (1B1.3A) mAb, which was purified from hybridoma cell culture supernatant (American Type Culture Collection); 0.5 mg anti–TGF-β (1D11) Ab (R&D Systems); and 0.25 mg anti–CTLA-4 (UC10-4F10-11) Ab (Bio-XCell, Lebanon, NH), as well as proper IgG controls (rat, mouse, and hamster, respectively), all from Jackson ImmunoResearch Laboratories.

Statistical analysis

Results were expressed as mean ± SD. Differences between groups were examined for statistical significance, using the Student *t* test.

Results

Pathogen-specific Tregs are activated and expand upon VV infection

To study the behavior of pathogen-specific Tregs in response to an acute infection in vivo, we used a model of influenza HA-specific Tregs in response to infection with VV-HA. HA-specific Tregs were derived from 6.5 HA-TCR transgenic mice ($Thy1.1^+$) that express a TCR recognizing an $I\text{-}E^d$–restricted HA epitope (^{110}SFERFEIFPKE^{120}) (31, 35–37). We first characterized the activation and expansion of HA-specific Tregs following VV-HA infection. HA-specific Tregs ($6.5^+CD4^+CD25^+$) were purified from naive 6.5 HA-TCR transgenic mice by FACS sorting. The sorted HA-specific Treg population was consistently >85% $Foxp3^+$ (data not shown). The 1×10^5 $Thy1.1^+$, purified HA-specific Tregs or non-Tregs ($6.5^+CD4^+CD25^-$) were transferred into congenic B10.D2 mice ($Thy1.2^+$). Mice were subsequently infected with VV-HA (2×10^6 PFU) i.p. or left uninfected as a control. At 7 d post infection, splenocytes were analyzed for clonal expansion of the HA-specific Treg ($Thy1.1^+CD4^+Foxp3^+$) or non-Treg ($Thy1.1^+CD4^+Foxp3^-$) population. Of total lymphocytes, 0.47% were clonotypic Tregs (Fig. 1A, 1B), which represented ~50-fold expansion compared with that of the mock-infected control mice (Fig. 1A). This expansion was less than that of the clonotypic non-Tregs, which represented 2.9% of the total lymphocytes (~290-fold expansion) (Fig. 1A, 1B). Despite expansion, very few clonotypic Tregs produced IFN-γ, compared with the 24% of the non-Treg population that were IFN-γ^+ (Fig. 1B). In contrast, no $Foxp3^+$ cells were detected in the non-Treg population (Fig. 1B). Similar degrees of expansion for both Treg and non-Treg populations were also found in other lymphoid tissues, including mesenteric and peripheral lymph nodes (data not shown).

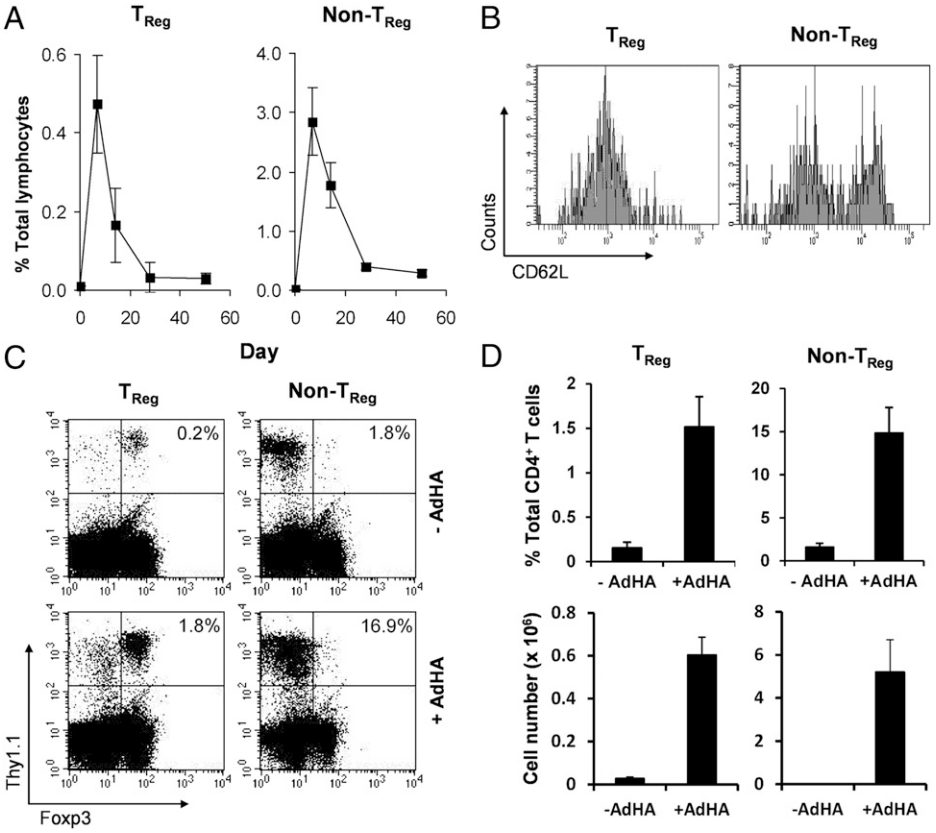

FIGURE 2. Activated pathogen-specific Tregs undergo contraction to form a memory population after resolution of infection. Purified naive HA-specific Tregs or non-Tregs ($Thy1.1^+$) were transferred into B10.D2 mice ($Thy1.2^+$), which were subsequently infected with VV-HA or left uninfected as a control. (**A**) At 7, 14, 28, and 50 d post infection, splenocytes were stained with anti-CD4, anti-Thy1.1, and anti-Foxp3, and the mean percentage of Tregs ($CD4^+$ $Thy1.1^+Foxp3^+$) or non-Tregs ($CD4^+Thy1.1^+Foxp3^-$) among total lymphocytes was plotted with the standard deviations included. (**B**) At 50 d post infection, splenocytes were stained with anti-CD62L, anti-CD4, anti-Thy1.1, and anti-Foxp3. Events were gated on $CD4^+Thy1.1^+Foxp3^+$ (Treg) or $CD4^+$ $Thy1.1^+Foxp3^-$ (non-Treg). (**C** and **D**) At 50 d post infection, mice were rechallenged with Ad-HA (+AdHA) or left uninfected as a control (−AdHA). At 4 d after rechallenge, splenocytes were stained with anti-CD4, anti-Thy1.1, and anti-Foxp3. The percentage of $CD4^+Thy1.1^+Foxp3^+$ (Treg) or $CD4^+$ $Thy1.1^+Foxp3^-$ (non-Treg) among total $CD4^+$ T cell is indicated (C). The mean percentages of Treg and non-Treg among total $CD4^+$ T cells, as well as their absolute cell numbers, were plotted with the standard deviations included (D). Results are representative of three independent experiments.

We next analyzed the phenotype of clonotypic Tregs after VV-HA infection. Similar to HA-specific non-Tregs, HA-specific Tregs downregulated CD62L, compared with naive controls (Fig. 1C). However, unlike non-Treg $CD4^+$ T cells, which upregulated CD44 upon infection (Fig. 1C), HA-specific Tregs exhibited high levels of CD44 expression even before VV-HA infection, and no obvious changes were observed post infection (Fig. 1C). This finding is consistent with the idea that Tregs are Ag experienced, as their selection in the thymus requires intermediate- to high-affinity TCR:peptide ligand interactions (35, 38). Collectively, these results show that pathogen-specific Tregs can be activated and expand following an acute viral infection. To further confirm that $Foxp3^+$ Tregs are capable of expanding upon VV infection in vivo, we intercrossed HA-TCR transgenic mice with Foxp3-GFP knockin mice, and similar results were obtained when 6.5^+CD4^+Foxp3-GFP^+ Tregs were used for adoptive transfer experiments followed by infection with VV-HA (Fig. 1D).

Activated Tregs undergo contraction to form a memory population

We next examined the fate of activated Tregs following the peak of clonal expansion at day 7. The majority of activated pathogen-specific Tregs underwent contraction after resolution of the infection, and only a small fraction (~5%) survived the contraction to form a stable memory population by day 28, which persisted through day 50 (Fig. 2A). This situation was similar to the formation of non-Treg memory $CD4^+$ T cells in vivo (Fig. 2A). On the basis of homing characteristics and effector functions, at least two subsets of memory T cells have been described for both $CD4^+$ and $CD8^+$ T cells (39): central memory T cells (T_{CM}) that express CD62L and effector memory T cells (T_{EM}) that lack CD62L. Indeed, non-Treg memory $CD4^+$ T cells displayed both the $CD62L^{lo}$ (T_{EM}) and $CD62L^{hi}$ (T_{CM}) populations. However, the memory Tregs were almost entirely $CD62L^{lo}$, corresponding to a T_{EM} phenotype (Fig. 2B).

One central hallmark of memory T cells is rapid recall expansion upon a secondary Ag challenge (40). To determine whether the memory Tregs also possessed this salient memory quality, mice that had received clonotypic Tregs, and were infected with VV-HA 50 d before, were rechallenged with Ad-HA i.v. At 4 d after rechallenge, memory Tregs rapidly expanded (~10-fold expansion compared with that of nonboosted mice; Fig. 2C, 2D). This fold expansion was similar to that of the non-Treg memory $CD4^+$ T cells (Fig. 2C, 2D). Thus, these pathogen-specific memory Tregs can also rapidly expand upon a secondary challenge. Taken together, these results suggest that a stable population of Tregs with memory characteristics can develop after resolution of the infection.

Memory Tregs suppress non-Treg $CD4^+$ T cell expansion upon secondary challenges

We next investigated the role of pathogen-specific Tregs during primary and recall responses to an acute infection. We cotransferred $Thy1.1^+$, HA-specific Tregs (1×10^5) with non-Tregs (1×10^5), or HA-specific non-Tregs only (1×10^5), into congenic B10.

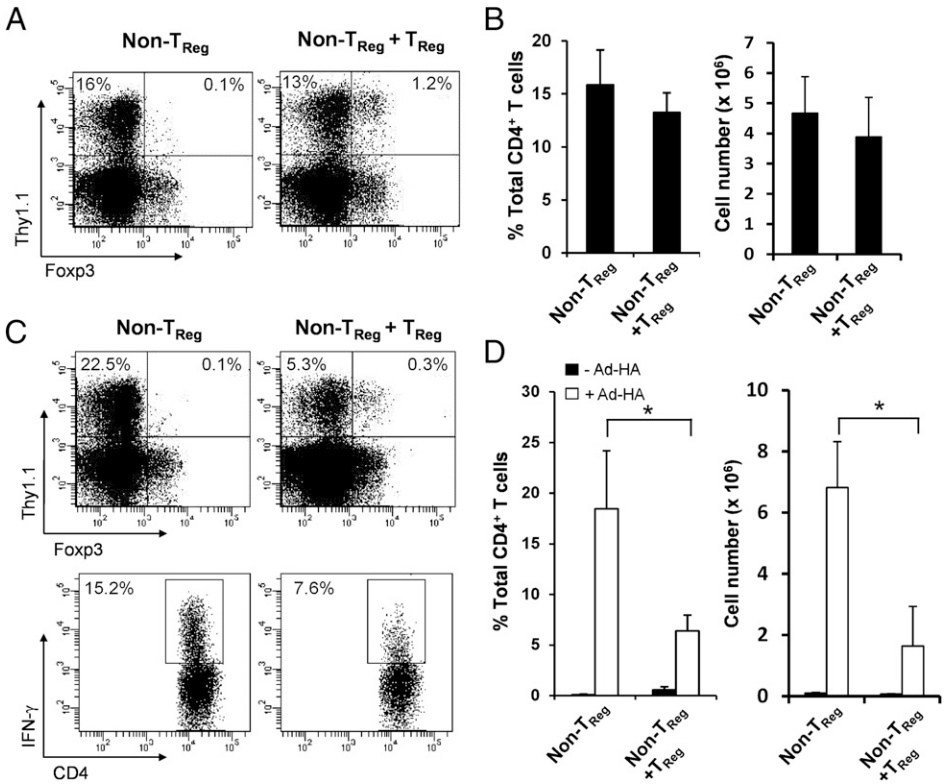

FIGURE 3. Memory Tregs suppress the expansion of non-Treg memory $CD4^+$ T cells in the liver. Purified naive HA-specific non-Tregs, with (Treg + Non-Treg) or without Tregs (Non-Treg), were transferred into B10.D2 mice, which were infected with VV-HA. (**A** and **B**) At 7 d post infection, splenocytes were harvested and stained with anti-CD4, anti-Thy1.1, and anti-Foxp3. The percentages of $CD4^+Thy1.1^+Foxp3^+$ Tregs and $CD4^+Thy1.1^+Foxp3^-$ non-Tregs within the $CD4^+$ T cell gate are indicated (A). The mean percentages of $CD4^+Thy1.1^+Foxp3^-$ non-Tregs among total $CD4^+$ T cells, as well as their absolute cell numbers, were plotted with the standard deviations included (B). (**C** and **D**) At 50 d post infection, mice were rechallenged with Ad-HA (+AdHA) or left uninfected as a control (−AdHA). At 4 d after rechallenge, splenocytes were harvested and analyzed for expansion and function. The percentages of $CD4^+Thy1.1^+Foxp3^+$ and $CD4^+Thy1.1^+Foxp3^-$ within the $CD4^+$ T cell gate are indicated (*top panels*). The percentage of IFN-γ^+ non-Tregs among $CD4^+Thy1.1^+Foxp3^-$ is indicated (*bottom panels*) (C). The mean percentages of $CD4^+Thy1.1^+Foxp3^-$ non-Tregs among total $CD4^+$ T cells, as well as their absolute cell numbers, were plotted with the standard deviations included (D). Results are representative of three independent experiments. $^*p < 0.001$.

D2 mice (Thy1.2$^+$), followed by infection with VV-HA. At 7 d post infection, we found that although the initial transfer was at a 1:1 ratio (non-Treg:Treg), clonotypic Tregs represented only ~10% of the donor (Thy1.1$^+$) population in mice that had received both Tregs and non-Tregs (data not shown). This is most likely due to the differences in expansion observed between clonotypic Tregs and non-Tregs in response to VV-HA infection (Fig. 1). We observed no significant difference in the expansion of non-Treg CD4$^+$ T cells, with or without the presence of clonotypic Tregs (Fig. 3A, 3B). In addition, no significant difference was noted in the percentage of IFN-γ^+ cells among clonotypic non-Tregs, with or without HA-specific Tregs (data not shown). Collectively, these results indicate that the presence of activated, pathogen-specific Tregs does not significantly affect the expansion and effector differentiation of non-Treg CD4$^+$ T cells during the primary response to VV-HA.

We then evaluated whether HA-specific memory Tregs could suppress the recall response of HA-specific non-Treg memory CD4$^+$ T cells. At 50 d post infection with VV-HA, the above mice that had received either Tregs with non-Tregs, or non-Tregs only, were rechallenged with Ad-HA. At 4 d after boost infection, mice were analyzed for the expansion of non-Treg CD4$^+$ T cells. Massive recall expansion of non-Treg memory CD4$^+$ T cells was detected in the absence of memory Tregs (Fig. 3C, 3D). In contrast, the extent of recall expansion of non-Treg CD4$^+$ T cells was significantly ($p < 0.001$) reduced in the presence of memory Tregs (Fig. 3C, 3D). In addition, a reduction was noted in the percentage of IFN-γ^+ cells among non-Treg CD4$^+$ T cells in the presence of memory Tregs (Fig. 3C). The differences in expansion were not due to differential contraction of non-Tregs in the presence of Tregs, as the percentage of non-Treg memory CD4$^+$ T cells was similar between both groups prior to Ag rechallenge (Fig. 3D). Thus, HA-specific memory Tregs suppress the expansion and effector function of HA-specific non-Treg memory CD4$^+$ T cells during an Ag recall response.

We next tested whether the observed function of memory Tregs could be confirmed in a different model of acute viral infection. In this experiment, we used a model of influenza viral infection that induces lung disease. Again, we cotransferred Thy1.1$^+$, HA-specific Tregs (1×10^5) with non-Tregs (1×10^5), or HA-specific non-Tregs only (1×10^5), into congenic B10.D2 mice (Thy1.2$^+$), followed by infection with influenza virus (4000 tissue culture-infective dose, at 50%) intranasally. At 7 d later, we evaluated the spleen (data not shown) and draining hilar lymph nodes for clonal expansion of HA-specific non-Tregs and Tregs. We observed no significant difference in the primary expansion of non-Treg CD4$^+$ T cells with or without the presence of clonotypic Tregs (Fig. 4A, 4B). In addition, no significant difference was observed in the percentage of IFN-γ^+ cells among clonotypic non-Tregs, with or without HA-specific Tregs (data not shown). Thus, similar to infection with VV-HA, the presence of activated, pathogen-specific Tregs does not affect the expansion or effector differentiation

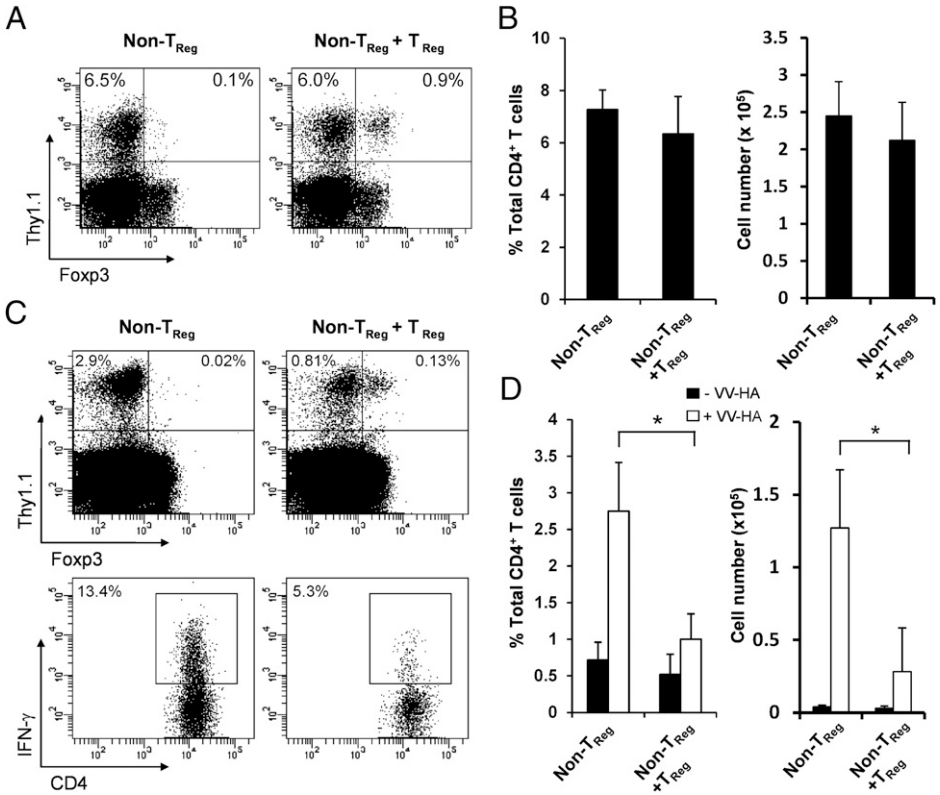

FIGURE 4. Memory Tregs suppress the expansion of non-Treg memory CD4$^+$ T cells in the lungs. Purified naive HA-specific non-Tregs, with (Treg + Non-Treg) or without Tregs (Non-Treg), were transferred into B10.D2 mice, which were infected with influenza virus. (**A** and **B**) At 7 d post infection, draining hilar lymphocytes were harvested and stained with anti-CD4, anti-Thy1.1, and anti-Foxp3. The percentages of CD4$^+$Thy1.1$^+$Foxp3$^+$ and CD4$^+$Thy1.1$^+$Foxp3$^-$ within the CD4$^+$ T cell gate are indicated (A). The mean percentages of CD4$^+$Thy1.1$^+$Foxp3$^-$ non-Tregs among total CD4$^+$ T cells, as well as their absolute cell numbers, were plotted with the standard deviations included (B). (**C** and **D**) At 50 d post infection, mice were rechallenged with VV-HA (+VV-HA) or left uninfected as a control (−VV-HA). At 5 d after rechallenge, draining hilar lympocytes were harvested and analyzed for expansion and function. The percentages of CD4$^+$Thy1.1$^+$Foxp3$^+$ and CD4$^+$Thy1.1$^+$Foxp3$^-$ within the CD4$^+$ T cell gate are indicated (*top panels*) and the percentage of IFN-γ^+ non-Tregs among CD4$^+$Thy1.1$^+$Foxp3$^-$ is indicated (*bottom panels*) (C). The mean percentages of CD4$^+$Thy1.1$^+$Foxp3$^-$ non-Tregs among total CD4$^+$ T cells, as well as their absolute cell numbers, were plotted with the standard deviations included (D). Results are representative of three independent experiments. *$p < 0.001$.

of non-Treg $CD4^+$ T cells during the primary response to influenza virus.

We then evaluated whether HA-specific memory Tregs formed following influenza priming would suppress activation of HA-specific memory non-Tregs after Ag rechallenge with VV-HA. At 50 d post infection with influenza, the above mice that had received either Tregs with non-Tregs, or non-Tregs only, were rechallenged with VV-HA (5×10^5 PFU) intranasally. At 5 d after boost infection, mice were analyzed for the expansion of non-Treg $CD4^+$ T cells. The recall expansion of non-Treg memory cells was significantly ($p < 0.001$) reduced in the presence of memory Tregs (Fig. 4C, 4D). We also observed a significant reduction in IFN-γ^+ cells among clonotypic non-Tregs in the presence of memory Tregs (Fig. 4C). Taken together, the results from two different models of acute viral infection support our conclusion that memory Tregs suppress the expansion and function of non-Treg $CD4^+$ T cell expansion during a recall response.

Memory Tregs control the extent of immunopathological effects during recall responses

What, then, is the biological significance of memory Treg-mediated suppression on non-Treg $CD4^+$ T cells during a recall response in vivo? Because of the vigorous expansion of non-Treg $CD4^+$ T cells that occurred during a recall response, we hypothesized that memory Treg-mediated suppression may prevent the collateral damage that could result from such a robust response. To test this hypothesis, we examined immunopathological conditions in mice with or without memory Tregs. For the first model, we selected liver tissues for histopathological examination because studies have shown that the liver is the primary target organ for adenoviral vectors (41). Again, we cotransferred HA-specific Tregs with HA-specific non-Tregs, or HA-specific non-Tregs alone, into B10.D2 mice, followed by VV-HA infection. At 50 d post infection, mice were rechallenged with Ad-HA. At 4 d after rechallenge, liver tissues were evaluated for tissue effects. We found widespread severe immunopathological changes and tissue damage characterized by hepatocellular degeneration, focal necrosis, and periportal infiltration in mice that received only non-Treg $CD4^+$ T cells (Fig. 5A, 5B). Immunohistochemical staining revealed that the portal inflammation mainly consisted of infiltrating $CD4^+$ T cells (Fig. 5A, 5C). By contrast, the overall immunopathological condition was diminished, with a significant ($p < 0.001$) reduction of periportal infiltrating $CD4^+$ T cells in the presence of memory Tregs (Fig. 5). This reduction was accompanied by a significant accumulation of memory Tregs in the liver upon rechallenge (Fig. 5D). These results suggest that memory Treg-mediated suppression prevents overwhelming immunopathological changes during a robust recall response. However, the

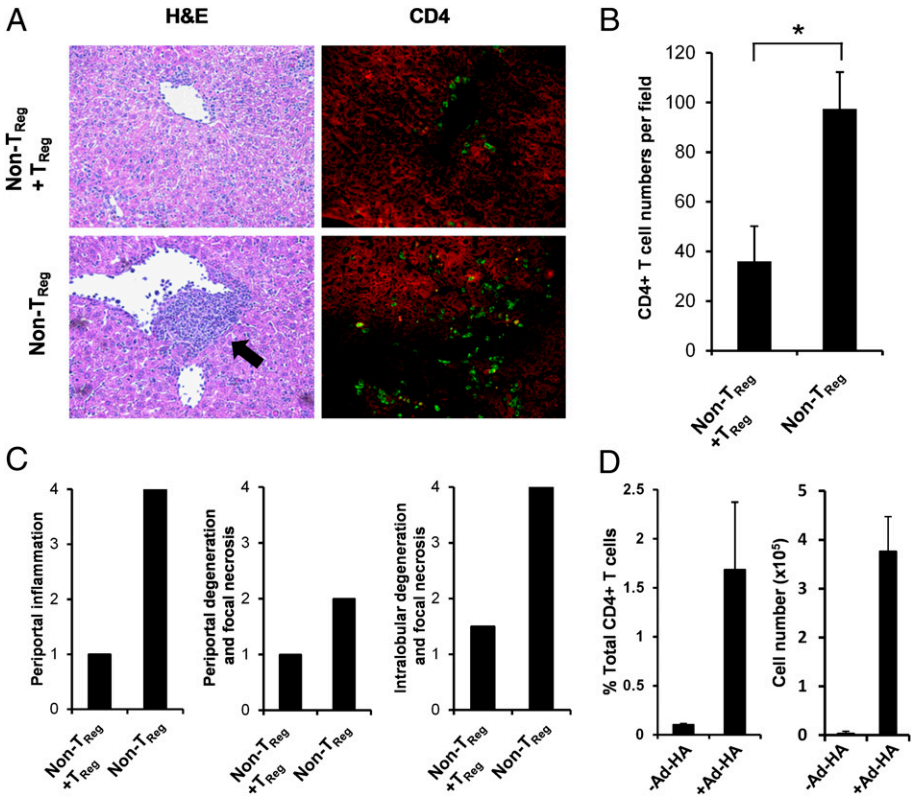

FIGURE 5. Memory Tregs control the extent of liver immunopathological effects during a recall response. Purified naive HA-specific non-Tregs, with (Treg + Non-Treg) or without Tregs (Non-Treg), were transferred into B10.D2 mice, which were infected with VV-HA. At 50 d post infection, mice were rechallenged with Ad-HA, and 4 d after rechallenge, liver tissues were harvested and examined for histopathological changes and infiltrating lymphocytes. (**A**) Paraffin sections were stained with H&E (*left panel*), and cryosections were stained with anti-CD4 (green) and anti-HA (red) by immunofluorescence (*right panel*). Original magnification ×100. The arrowhead indicates periportal infiltration. (**B**) Paraffin sections were stained with H&E and evaluated for evidence of pathological changes by light microscopic examination. Sections were characterized with respect to periportal inflammation, periportal degeneration and focal necrosis, and intralobular degeneration and focal necrosis. Extent of pathological damage was scored from 0 (none) to 4 (severe). (**C**) The mean numbers of $CD4^+$ T cells per field of view were plotted with the standard deviations included. *$p < 0.001$. (**D**) Accumulation of Tregs at the site of infection following Ag rechallenge. Purified naive HA-specific non-Tregs and Tregs were transferred into B10.D2 mice, which were infected with VV-HA i.p. At 50 d post infection, mice were rechallenged with Ad-HA (+Ad-HA) or left uninfected as a control (−Ad-HA). At 4 d after rechallenge, lymphocytes were harvested from the liver and analyzed for HA-specific Tregs. The mean percentages of HA-specific Tregs among total $CD4^+$ T cells, as well as their absolute cell numbers, were plotted with the standard deviations included. Results are representative of three independent experiments.

expression of HA in the liver was similar in mice, with or without memory Tregs, at day 4 post rechallenge (Fig. 5A), and it became undetectable by day 10 post rechallenge (data not shown), suggesting that the presence of memory Tregs did not appear to affect the clearance of HA in the liver.

We then assessed immunopathological changes in the second model of infection with influenza virus. Again, we cotransferred HA-specific Tregs with HA-specific non-Tregs, or HA-specific non-Tregs alone, into congenic B10.D2 mice, followed by influenza infection. At 50 d post infection, mice were rechallenged with VV-HA. At 5 d after rechallenge, lung tissues were evaluated for histopathological effects. We found severe immunopathological changes and tissue damage characterized by perivascular and peribronchial infiltration mainly consisting of infiltrating $CD4^+$ T cells in mice that received non-Tregs alone (Fig. 6A). By contrast, the overall immunopathological condition was diminished, with a reduction of perivascular and peribronchial infiltration in the presence of memory Tregs (Fig. 6B). Collectively, these results suggest that memory Treg-mediated suppression prevents overwhelming immunopathological changes during a robust recall response.

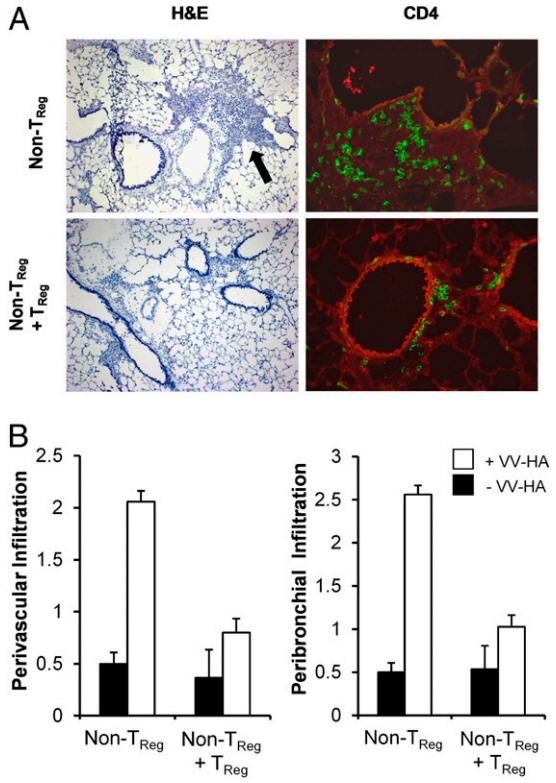

FIGURE 6. Memory Tregs control the extent of lung immunopathological changes during a recall response. Purified naive HA-specific non-Tregs, with (Treg + Non-Treg) or without Tregs (Non-Treg), were transferred into B10.D2 mice, which were infected with influenza virus. At 50 d post infection, mice were rechallenged with VV-HA. At 5 d after rechallenge, lung tissues were harvested and analyzed for immunopathological effects. (**A**) Cryosections were stained with hematoxylin (*left panel*) or with anti-CD4 (green) by immunofluorescence (*right panel*). Original magnification ×100. The arrowhead indicates peribronchial infiltration. (**B**) Cryosections were stained with hematoxylin and evaluated for evidence of pathological changes by light microscopic examination. Sections were characterized with respect to perivascular and peribronchial infiltration. Extent of pathological damage was scored from 0 (none) to 4 (severe). The mean score for 10 fields of view from at least three cryosections per group was graphed with the SE included. Results are representative of three independent experiments.

Suppression by memory Tregs is mediated through IL-10

We next investigated what is responsible for memory Treg-mediated suppression on non-Treg $CD4^+$ T cells during the recall response. Because CTLA-4, IL-10, and TGF-β have been implicated in Treg-mediated suppression in vivo (14), we examined the effects of CTLA-4, IL-10, and TGF-β blockade on the recall response. We transferred HA-specific non-Tregs with Tregs into congenic B10.D2 mice, which then received influenza virus intranasally. At 50 d following infection, mice were treated with anti–CTLA-4, anti–IL-10 receptor (IL-10R), anti–TGF-β, or a control IgG, followed by a secondary challenge with VV-HA. At 5 d later, mice were analyzed for the expansion of non-Treg $CD4^+$ T cells. We found that only IL-10R blockade led to significantly ($p < 0.01$) enhanced expansion of non-Treg $CD4^+$ T cells (Fig. 7A, 7B) and exacerbation of lung disease (Fig. 7C) in the presence of memory Tregs, but not in the absence of memory Tregs, suggesting IL-10 is responsible for memory Treg-mediated suppression on non-Treg $CD4^+$ T cells. We further found that although quiescent memory Tregs produced little IL-10, they produced much higher levels of IL-10 upon Ag rechallenge (Fig. 7D, 7E). Taken together, these data indicate that memory Treg-mediated suppression on non-Treg $CD4^+$ T cells and immunopathological effects during the recall response are mediated by IL-10.

Discussion

In this study, we have examined the kinetics and function of pathogen-specific Tregs in two different models of acute viral infection. Our work reveals a previously unknown memory Treg population that develops following acute viral infections in vivo. We show that memory Tregs suppress the expansion and effector function of non-Treg memory $CD4^+$ T cells upon secondary challenge. These memory Tregs play a critical role in controlling excessive immunopathological changes that occur during the recall expansion of non-Treg memory $CD4^+$ T cells upon secondary challenge. Furthermore, we demonstrate that these memory Tregs secrete high levels of IL-10 upon Ag rechallenge and that the function of memory Tregs is mediated by an IL-10–dependent mechanism.

Our observation that Ag-specific Tregs expanded in response to acute VV or influenza viral infections is consistent with previous observations in models of HSV and *Leishmania* infections (29, 30, 42, 43), but stands in contrast to a model of *Listeria* infection (44). In this model, infection with *Listeria monocytogenes* led to expansion of *L. monocytogenes*-specific $CD4^+Foxp3^-$ T cells, but *L. monocytogenes*-specific $CD4^+Foxp3^+$ Tregs. It is not entirely clear what contributes to the discrepancy, but it could be related to different pathogens, routes of administration, and experimental conditions.

Upon viral infections, non-Treg $CD4^+$ and $CD8^+$ T cells expand and then contract, with only a small fraction (5–10%) surviving to form the stable memory population (39). Following infection with VV-HA, we observed that pathogen-specific Tregs behave with similar kinetics to non-Treg $CD4^+$ T cells, albeit with a lower initial expansion. The memory Tregs that survive the contraction phase can also respond rapidly to secondary Ag rechallenge. However, unlike non-Treg memory $CD4^+$ T cells that consist of both $CD62L^{lo}$, effector memory (T_{EM}), and $CD62L^{hi}$, central memory (T_{CM}), populations, these memory Tregs display almost exclusively a $CD62L^{lo}$, T_{EM} phenotype. The expression of CD62L on T_{CM} allows them to home to lymph nodes efficiently and differentiate into effector cells upon Ag restimulation. In contrast, owing to lack of lymph node homing receptors, CD62L, T_{EM} migrate into nonlymphoid tissues and display immediate effector functions for the rapid control of invading pathogens. The T_{EM}

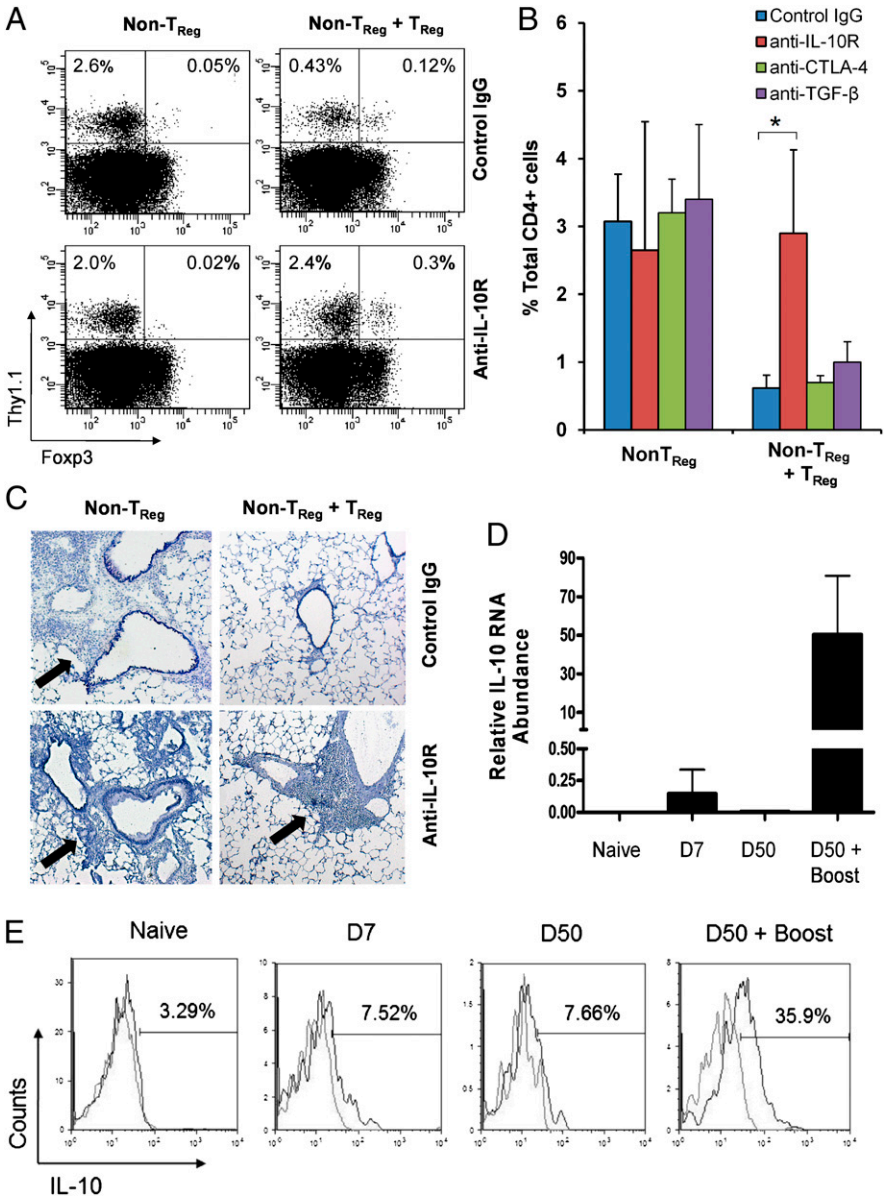

FIGURE 7. Memory Tregs suppress the expansion of non-Treg memory CD4$^+$ T cells via IL-10. (**A**–**C**) Purified naive HA-specific non-Tregs, with (Treg + Non-Treg) or without Tregs (Non-Treg), were transferred into B10.D2 mice and infected with influenza virus. At 50 d post infection, mice received anti–IL-10R, anti–CTLA-4, anti–TGF-β, or a control IgG i.v. 6 h prior to infection with VV-HA and again 2 d later. At 5 d following rechallenge, draining hilar lymph nodes and lung tissue were harvested for analysis. (A) Hilar lymphocytes were harvested and stained with anti-CD4, anti-Thy1.1, and anti-Foxp3. The percentages of CD4$^+$Thy1.1$^+$Foxp3$^+$ Tregs and CD4$^+$Thy1.1$^+$ Foxp3$^-$ non-Tregs among total CD4$^+$ T cells are indicated. (B) The mean percentages of CD4$^+$Thy1.1$^+$Foxp3$^-$ non-Tregs among total CD4$^+$ T cells were plotted with the standard deviations included. *$p < 0.01$. (C) Cryosections of lung tissue were stained with hematoxylin. Original magnification ×100. Arrowheads indicate peribronchial infiltration. (**D** and **E**) Purified naive HA-specific Tregs (Thy1.1$^+$) were transferred into B10.D2 mice and infected with influenza virus or left uninfected (naive). HA-specific Tregs were analyzed 7 (D7) and 50 (D50) d post infection, as well as 5 d after Ag rechallenge (D50 + boost), which was done 50 d after initial infection. (D) HA-specific Tregs were purified by staining pooled cells from the lymph nodes and spleen with anti-CD4 and anti-Thy1.1 to sort CD4$^+$ Thy1.1$^+$ Tregs. mRNA was isolated from naive, D7, D50, and D50 + boost Tregs, and the levels of IL-10 and β-actin were measured by real-time RT-PCR. The relative quantities of mRNA, normalized to β-actin, from a representative sample are indicated. (E) HA-specific Tregs were stained with anti-CD4, anti-Thy1.1, anti-Foxp3, and anti–IL-10 (intracellular, black) or isotype control (gray). The percentages of CD4$^+$Thy1.1$^+$Foxp3$^+$ cells that are IL-10$^+$ are indicated. Results are representative of three independent experiments.

phenotype of the memory Tregs may allow them to migrate quickly into nonlymphoid tissues, such as liver and lung, to exert immediate control of collateral tissue damage (39). Indeed, we found rapid accumulation of memory Tregs in the liver upon Ag rechallenge (Fig. 5D).

Our observation that memory Tregs suppress the expansion and effector function of non-Treg memory CD4$^+$ T cells and play a critical role in controlling excessive immunopathological effects during the recall response, further supports the growing body of evidence that Tregs are essential in preventing immunopathological disorders in various models of bacterial, viral, parasitic, and fungal infections (26–28, 45). Inhibition of immunopathological changes during a recall response may be of particular importance because of the rapid and robust expansion of memory non-Tregs. Indeed, we observed much greater immunopathological effects in the liver or lungs during a recall response than during a primary response (A.M. Sanchez and Y. Yang, unpublished observations).

Multiple mechanisms have been proposed for Treg-mediated suppression in vivo, including the production of immunosuppressive cytokines such as IL-10 and TGF-β, direct cell–cell contact, and inhibition of APC function (14). In this article, we have provided in vivo evidence that IL-10R blockade significantly reduces the ability of memory Tregs to suppress the recall expansion of non-Treg CD4$^+$ T cells and the attendant immunopathological changes, and that memory Tregs produced high levels of IL-10 upon rechallenge, suggesting that IL-10 is responsible for memory Treg-mediated suppression. It remains to be defined how IL-10 suppresses non-Treg CD4$^+$ T cell responses and whether other mechanisms of Treg-mediated suppression are also used. Thus, it would be important to address these questions in the future.

In this study, no obvious Treg-mediated suppression on the expansion of non-Treg CD4$^+$ T cells was detected during the primary response to VV or influenza in vivo. Our results are in line with the observations in models of infection with *Pseudomonas* and *Trypanosoma* (46, 47), but are in contrast to the model of HSV infections (42, 43), as well as the model of peptide IFA immunization (48). The reasons for the discrepancy are not entirely clear but may be due to different experimental models and conditions. In the studies with HSV infection, the polyclonal population of Tregs was deleted, as opposed to addition of Ag-specific Tregs in our study, which could affect the overall suppressive capability of Tregs. In addition, different infections and immu-

nizations could elicit different inflammatory milieu and/or innate immune response, both of which have been suggested to play a role in overcoming Treg-mediated suppression (32, 49, 50).

We observed a difference in the suppressive ability of naive or activated Tregs during the primary response versus memory Tregs during the recall response. This difference is not likely due to changes in Treg frequency between the primary and recall responses, as the percentage of Tregs among total Ag-specific T cells remains similar during the initial priming and the recall response. Similarly, this difference is not likely a result of different viruses used between the priming and recall response because VV has been used in both settings in our models. Rather, our data suggest that the increased suppressive potential of memory Tregs is due to the ability to produce markedly elevated levels of IL-10 upon rechallenge. Thus, a qualitative difference exists between memory and naive Tregs in the ability to suppress non-Tregs, and this qualitative difference is reflected in their ability to rapidly produce high levels of IL-10 in response to Ag stimulation. The underlying mechanism leading to this qualitative gain by memory Tregs requires further investigation.

In conclusion, we have shown that pathogen-specific Tregs expand and contract following acute viral infections, with a small population developing into the memory Treg pool. These memory Tregs suppress memory non-Tregs upon a secondary challenge. The suppression by memory Tregs is critical to the control of immunopathological changes that occur during the recall response as a result of robust non-Treg expansion. Finally, we demonstrate that suppression by memory Tregs results, at least in part, from their ability to produce high levels of IL-10 during the recall response. Our work reveals a previously unknown memory Treg population that develops following acute viral infection in vivo and may help in the design of effective strategies to circumvent excessive immunopathological changes during a recall response.

Acknowledgments

We thank Dr. H. von Boehmer for providing 6.5 HA-TCR transgenic mice.

Disclosures

The authors have no financial conflicts of interest.

References

1. Baecher-Allan, C., V. Viglietta, and D. A. Hafler. 2004. Human CD4+CD25+ regulatory T cells. *Semin. Immunol.* 16: 89–98.
2. Shevach, E. M. 2002. CD4+ CD25+ suppressor T cells: more questions than answers. *Nat. Rev. Immunol.* 2: 389–400.
3. McHugh, R. S., M. J. Whitters, C. A. Piccirillo, D. A. Young, E. M. Shevach, M. Collins, and M. C. Byrne. 2002. CD4(+)CD25(+) immunoregulatory T cells: gene expression analysis reveals a functional role for the glucocorticoid-induced TNF receptor. *Immunity* 16: 311–323.
4. Shimizu, J., S. Yamazaki, T. Takahashi, Y. Ishida, and S. Sakaguchi. 2002. Stimulation of CD25(+)CD4(+) regulatory T cells through GITR breaks immunological self-tolerance. *Nat. Immunol.* 3: 135–142.
5. Yamaguchi, T., K. Hirota, K. Nagahama, K. Ohkawa, T. Takahashi, T. Nomura, and S. Sakaguchi. 2007. Control of immune responses by antigen-specific regulatory T cells expressing the folate receptor. *Immunity* 27: 145–159.
6. Hori, S., T. Nomura, and S. Sakaguchi. 2003. Control of regulatory T cell development by the transcription factor Foxp3. *Science* 299: 1057–1061.
7. Fontenot, J. D., M. A. Gavin, and A. Y. Rudensky. 2003. Foxp3 programs the development and function of CD4+CD25+ regulatory T cells. *Nat. Immunol.* 4: 330–336.
8. Khattri, R., T. Cox, S. A. Yasayko, and F. Ramsdell. 2003. An essential role for Scurfin in CD4+CD25+ T regulatory cells. *Nat. Immunol.* 4: 337–342.
9. von Boehmer, H. 2005. Mechanisms of suppression by suppressor T cells. *Nat. Immunol.* 6: 338–344.
10. Sakaguchi, S. 2004. Naturally arising CD4+ regulatory T cells for immunologic self-tolerance and negative control of immune responses. *Annu. Rev. Immunol.* 22: 531–562.
11. Ghiringhelli, F., C. Ménard, M. Terme, C. Flament, J. Taieb, N. Chaput, P. E. Puig, S. Novault, B. Escudier, E. Vivier, et al. 2005. CD4+CD25+ regulatory T cells inhibit natural killer cell functions in a transforming growth factor-beta-dependent manner. *J. Exp. Med.* 202: 1075–1085.
12. Miyara, M., and S. Sakaguchi. 2007. Natural regulatory T cells: mechanisms of suppression. *Trends Mol. Med.* 13: 108–116.
13. Lim, H. W., P. Hillsamer, A. H. Banham, and C. H. Kim. 2005. Cutting edge: direct suppression of B cells by CD4+ CD25+ regulatory T cells. *J. Immunol.* 175: 4180–4183.
14. Shevach, E. M. 2009. Mechanisms of foxp3+ T regulatory cell-mediated suppression. *Immunity* 30: 636–645.
15. Bennett, C. L., J. Christie, F. Ramsdell, M. E. Brunkow, P. J. Ferguson, L. Whitesell, T. E. Kelly, F. T. Saulsbury, P. F. Chance, and H. D. Ochs. 2001. The immune dysregulation, polyendocrinopathy, enteropathy, X-linked syndrome (IPEX) is caused by mutations of FOXP3. *Nat. Genet.* 27: 20–21.
16. Chatila, T. A., F. Blaeser, N. Ho, H. M. Lederman, C. Voulgaropoulos, C. Helms, and A. M. Bowcock. 2000. JM2, encoding a fork head-related protein, is mutated in X-linked autoimmunity-allergic disregulation syndrome. *J. Clin. Invest.* 106: R75–R81.
17. Wildin, R. S., F. Ramsdell, J. Peake, F. Faravelli, J. L. Casanova, N. Buist, E. Levy-Lahad, M. Mazzella, O. Goulet, L. Perroni, et al. 2001. X-linked neonatal diabetes mellitus, enteropathy and endocrinopathy syndrome is the human equivalent of mouse scurfy. *Nat. Genet.* 27: 18–20.
18. Viglietta, V., C. Baecher-Allan, H. L. Weiner, and D. A. Hafler. 2004. Loss of functional suppression by CD4+CD25+ regulatory T cells in patients with multiple sclerosis. *J. Exp. Med.* 199: 971–979.
19. Lindley, S., C. M. Dayan, A. Bishop, B. O. Roep, M. Peakman, and T. I. Tree. 2005. Defective suppressor function in CD4(+)CD25(+) T-cells from patients with type 1 diabetes. *Diabetes* 54: 92–99.
20. Ehrenstein, M. R., J. G. Evans, A. Singh, S. Moore, G. Warnes, D. A. Isenberg, and C. Mauri. 2004. Compromised function of regulatory T cells in rheumatoid arthritis and reversal by anti-TNFalpha therapy. *J. Exp. Med.* 200: 277–285.
21. Curotto de Lafaille, M. A., and J. J. Lafaille. 2002. CD4(+) regulatory T cells in autoimmunity and allergy. *Curr. Opin. Immunol.* 14: 771–778.
22. Kang, S. M., Q. Tang, and J. A. Bluestone. 2007. CD4+CD25+ regulatory T cells in transplantation: progress, challenges and prospects. *Am. J. Transplant.* 7: 1457–1463.
23. Wang, H. Y., and R. F. Wang. 2007. Regulatory T cells and cancer. *Curr. Opin. Immunol.* 19: 217–223.
24. Mills, K. H. 2004. Regulatory T cells: friend or foe in immunity to infection? *Nat. Rev. Immunol.* 4: 841–855.
25. Belkaid, Y., and B. T. Rouse. 2005. Natural regulatory T cells in infectious disease. *Nat. Immunol.* 6: 353–360.
26. Suvas, S., A. K. Azkur, B. S. Kim, U. Kumaraguru, and B. T. Rouse. 2004. CD4+ CD25+ regulatory T cells control the severity of viral immunoinflammatory lesions. *J. Immunol.* 172: 4123–4132.
27. McKinley, L., A. J. Logar, F. McAllister, M. Zheng, C. Steele, and J. K. Kolls. 2006. Regulatory T cells dampen pulmonary inflammation and lung injury in an animal model of *pneumocystis* pneumonia. *J. Immunol.* 177: 6215–6226.
28. Hesse, M., C. A. Piccirillo, Y. Belkaid, J. Prufer, M. Mentink-Kane, M. Leusink, A. W. Cheever, E. M. Shevach, and T. A. Wynn. 2004. The pathogenesis of schistosomiasis is controlled by cooperating IL-10-producing innate effector and regulatory T cells. *J. Immunol.* 172: 3157–3166.
29. Suffia, I. J., S. K. Reckling, C. A. Piccirillo, R. S. Goldszmid, and Y. Belkaid. 2006. Infected site-restricted Foxp3+ natural regulatory T cells are specific for microbial antigens. *J. Exp. Med.* 203: 777–788.
30. Belkaid, Y., C. A. Piccirillo, S. Mendez, E. M. Shevach, and D. L. Sacks. 2002. CD4+CD25+ regulatory T cells control *Leishmania major* persistence and immunity. *Nature* 420: 502–507.
31. Huang, X., J. Zhu, and Y. Yang. 2005. Protection against autoimmunity in nonlymphopenic hosts by CD4+ CD25+ regulatory T cells is antigen-specific and requires IL-10 and TGF-beta. *J. Immunol.* 175: 4283–4291.
32. Yang, Y., C. T. Huang, X. Huang, and D. M. Pardoll. 2004. Persistent Toll-like receptor signals are required for reversal of regulatory T cell-mediated CD8 tolerance. *Nat. Immunol.* 5: 508–515.
33. Lin, K. L., Y. Suzuki, H. Nakano, E. Ramsburg, and M. D. Gunn. 2008. CCR2+ monocyte-derived dendritic cells and exudate macrophages produce influenza-induced pulmonary immune pathology and mortality. *J. Immunol.* 180: 2562–2572.
34. Yang, Y., H. C. Ertl, and J. M. Wilson. 1994. MHC class I-restricted cytotoxic T lymphocytes to viral antigens destroy hepatocytes in mice infected with E1-deleted recombinant adenoviruses. *Immunity* 1: 433–442.
35. Jordan, M. S., A. Boesteanu, A. J. Reed, A. L. Petrone, A. E. Holenbeck, M. A. Lerman, A. Naji, and A. J. Caton. 2001. Thymic selection of CD4+ CD25+ regulatory T cells induced by an agonist self-peptide. *Nat. Immunol.* 2: 301–306.
36. Apostolou, I., A. Sarukhan, L. Klein, and H. von Boehmer. 2002. Origin of regulatory T cells with known specificity for antigen. *Nat. Immunol.* 3: 756–763.
37. D'Cruz, L. M., and L. Klein. 2005. Development and function of agonist-induced CD25+Foxp3+ regulatory T cells in the absence of interleukin 2 signaling. *Nat. Immunol.* 6: 1152–1159.
38. Fontenot, J. D., J. P. Rasmussen, L. M. Williams, J. L. Dooley, A. G. Farr, and A. Y. Rudensky. 2005. Regulatory T cell lineage specification by the forkhead transcription factor foxp3. *Immunity* 22: 329–341.
39. Sallusto, F., J. Geginat, and A. Lanzavecchia. 2004. Central memory and effector memory T cell subsets: function, generation, and maintenance. *Annu. Rev. Immunol.* 22: 745–763.
40. Seder, R. A., and R. Ahmed. 2003. Similarities and differences in CD4+ and CD8+ effector and memory T cell generation. *Nat. Immunol.* 4: 835–842.
41. Wilson, J. M. 1996. Adenoviruses as gene-delivery vehicles. *N. Engl. J. Med.* 334: 1185–1187.

42. Suvas, S., U. Kumaraguru, C. D. Pack, S. Lee, and B. T. Rouse. 2003. CD4+ CD25+ T cells regulate virus-specific primary and memory CD8+ T cell responses. *J. Exp. Med.* 198: 889–901.
43. Toka, F. N., S. Suvas, and B. T. Rouse. 2004. CD4+ CD25+ T cells regulate vaccine-generated primary and memory CD8+ T-cell responses against herpes simplex virus type 1. *J. Virol.* 78: 13082–13089.
44. Ertelt, J. M., J. H. Rowe, T. M. Johanns, J. C. Lai, J. B. McLachlan, and S. S. Way. 2009. Selective priming and expansion of antigen-specific Foxp3− CD4+ T cells during *Listeria monocytogenes* infection. *J. Immunol.* 182: 3032–3038.
45. Montagnoli, C., A. Bacci, S. Bozza, R. Gaziano, P. Mosci, A. H. Sharpe, and L. Romani. 2002. B7/CD28-dependent CD4+CD25+ regulatory T cells are essential components of the memory-protective immunity to *Candida albicans*. *J. Immunol.* 169: 6298–6308.
46. Carrigan, S. O., Y. J. Yang, T. Issekutz, N. Forward, D. Hoskin, B. Johnston, and T. J. Lin. 2009. Depletion of natural CD4+CD25+ T regulatory cells with anti-CD25 antibody does not change the course of *Pseudomonas aeruginosa*-induced acute lung infection in mice. *Immunobiology* 214: 211–222.
47. Kotner, J., and R. Tarleton. 2007. Endogenous CD4(+) CD25(+) regulatory T cells have a limited role in the control of *Trypanosoma cruzi* infection in mice. *Infect. Immun.* 75: 861–869.
48. Klein, L., K. Khazaie, and H. von Boehmer. 2003. In vivo dynamics of antigen-specific regulatory T cells not predicted from behavior in vitro. *Proc. Natl. Acad. Sci. USA* 100: 8886–8891.
49. Pasare, C., and R. Medzhitov. 2003. Toll pathway-dependent blockade of CD4+CD25+ T cell-mediated suppression by dendritic cells. *Science* 299: 1033–1036.
50. Sutmuller, R. P., M. H. den Brok, M. Kramer, E. J. Bennink, L. W. Toonen, B. J. Kullberg, L. A. Joosten, S. Akira, M. G. Netea, and G. J. Adema. 2006. Toll-like receptor 2 controls expansion and function of regulatory T cells. *J. Clin. Invest.* 116: 485–494.